Research Article | Vol. 2, No. 5 / 15 May 2019 / OSA Continuum 1502

Interference filter based beam confinement for increased mechanical phase modulation

BENJAMIN EWERS* **AND RAOUL-AMADEUS LORBEER**

German Aerospace Center (DLR), Institute of Technical Physics, Pfaffenwaldring 38-40, 70569 Stuttgart, Germany
benjamin.ewers@dlr.de

Abstract: Modulating the phase or rather the optical path difference of a laser beam is a challenging task. Not too seldom limitations in optical path modulation bandwidth and optical path stroke limit the desired application. Approaches to compensate for these restrictions typically trade one parameter for another and vice versa. To avoid this trade off between parameters, an in-place beam folding would be desirable. Here, an approach based on a wedged optical light interference-filter trap (WOLIT) allows the increase of the optical path difference while maintaining a small and fast optical path modulator. We showed that with the WOLIT acting as an opto-mechanical-gearbox, mechanical mirror movements of 10 nm are sufficient to generate an optical path difference greater than 1 μm at a frequency of 100 kHz.

1. Introduction

Manipulating the optical phase or delaying an optical pulse is a common task in optical setups as e.g. stabilized optical cavities [1,2]. In optical cavities an ultra fast piezo can act as a phase shifter. For small phase strokes in the order of 200 nm it was shown that high bandwidths of 180 kHz are achievable [3,4]. To overcome the limitation in phase stroke, several other methods have been introduced. This includes fast linear oscillating delay lines [5], fast rotating optical delay lines [6,7], and fiber stretchers [8,9]. Furthermore, folded optical delay lines attempt to overcome the phase stroke limitation by temporarily trapping the optical light between two mirrors [10–12]. This folded beam path multiplies the generated phase stroke of an oscillating mirror by the number of passes. Due to the requirement of the spatial beam separation, the used mirrors are generally large compared to the beam diameter. These methods generally introduce large inertial masses which again limits the modulation bandwidth.

In this paper we demonstrate an optical folded beam path without the need of spatial separation. The size of the used optical elements may be as small as the beam diameter of the light source, which vice versa, reduces the necessary inertial masses. This wedged optical light interference-filter trap (WOLIT) overcomes both the former limitation in achievable optical phase stroke as well as the limitation in achievable modulation frequency bandwidth.

The core element of the WOLIT concept is a long pass edge interference filter. A long pass interference filter can be characterized by its edge-wavelength λ_e and transmission (T) edge steepness $dT/d\lambda$ [13]. Let us now assume a laser with a wavelength λ_l below λ_e. At an angle of incidence Θ equal to zero the coating will reflect the main portion of the laser light (Fig. 1 dotted line). Tilting the substrate of the edge filter is known to shift its transmission edge towards shorter wavelengths [13]. At visible wavelengths this is experienced as a change in color of a dichroic filter as e.g. can be seen at the facade of the Museum at Prairiefire in Kansas City. The wavelength shift is differently distinct for s- and p-polarized light. By choosing a linear polarized laser source, the mixing of two separate edges can be omitted and at the edge angle $\Theta_{e,\lambda=\lambda_e}$ the

#352770 https://doi.org/10.1364/OSAC.2.001502
Journal © 2019 Received 27 Nov 2018; revised 6 Mar 2019; accepted 6 Mar 2019; published 1 Apr 2019

OSA CONTINUUM

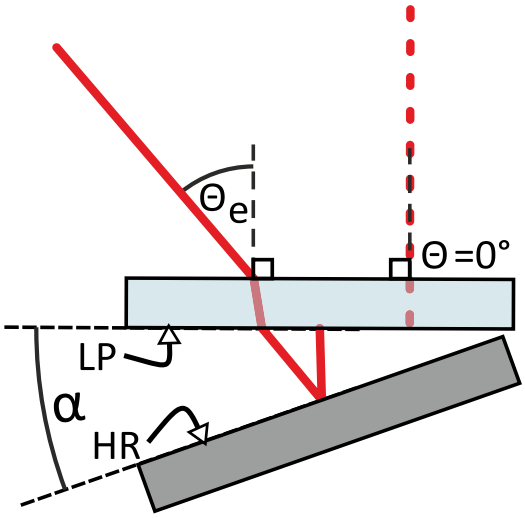

Fig. 1. Schematic arrangement of the WOLIT. Edge filter (light blue) and mirror (dark grey) with wedge angle α. Light beam with normal incidence (red dotted) and light beam with an incidence angle of Θ_e (red solid). Surfaces with long pass (LP) and highly reflective (HR) coating are indicated by their abberviations.

filter will begin to transmit the laser light (Fig. 1 solid line). This property allows to change between transmitting and reflecting the laser light by tilting the substrate by Θ_e.

Let us now assume the transmitted laser light to reach a second highly reflective mirror, redirecting the beam to its original direction. This would lead to a re-transmission of the laser light through the edge filter. Otherwise, it is also possible to redirect the laser light back to the interference filter with a tilted angle creating an effective Θ of 0 degrees. This will result in a reflection at the filter surface and therefore folding the beam back into itself (Fig. 1 solid line). The laser beam has been trapped for one additional round trip between both substrates. By choosing an appropriate wedge angle α between edge filter and mirror, a natural number N of round trips can be introduced as long as the first round trip changes Θ by the least necessary amount dictated by the transmission edge steepness.

This introduces beam folding, which for small distances d between filter and mirror, will essentially take place at the position of entrance into the WOLIT. Even though the WOLIT is quite similar to interferometric arrangements as e.g. the Fizeau interferometer or the air-wedged shearing interferometer, it is worth noting that an ideal WOLIT will only possess one entrance and one exit beam. All geometrically imposed interference effects will stay inside the optical assembly due to the choice of the reflective coatings.

Here we will focus on the optical path modulation capabilities of a WOLIT. In contrast to translational beam folding [11,12,14], in-place folding allows to use smaller beam diameters, small mirror diameters and small component distances. The only restriction is implied by the wedge angle which limits the incoming divergence angle of the beam. The beam itself neither needs to be displaced by its diameter nor to be collimated within the WOLIT which would increase the necessary distance d (Fig. 2 (b)).

The small distance d permits to limit the diameter of the mirror to a few millimeters. In a piezo mechanical arrangement [15] this allows to effectively keep diameters and therefore masses constant, while reducing the necessary displacement with beam folding. This results in the main advantage of the WOLIT arrangement, an overall improvement of responsiveness. To

OSA CONTINUUM

demonstrate the capabilities of a WOLIT, we chose to investigate the specific aspect of optical path difference (OPD) amplification in an experiment.

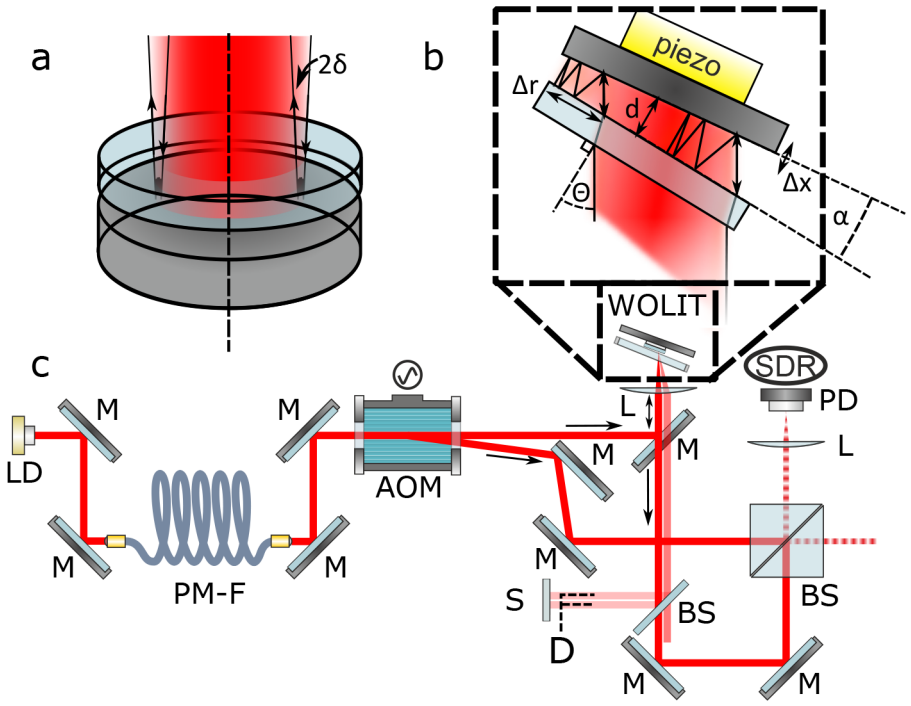

Fig. 2. The WOLIT. a) Side view. b) Front view. c) Experimental setup. Θ: angle of incidence; α: wedge angle; δ: angle enclosed between light beam and plane of symmetry; Δx: relative displacement of mirror relative to its surface normal; Δr; typical beam displacement; d: average distance; D: displacement between successive reflections after lens; LD: laser diode; M: mirror; PM-F: polarization maintaining single mode fiber; AOM: acousto optical modulator; L: lens; BS: beam sampler/splitter; S: screen; PD: photo diode; SDR: software defined radio

2. Materials and methods

The WOLIT consists of two opposing, essentially flat, glass substrates. In Fig. 2 (b) the incoming laser beam is displayed under an angle of incidence Θ. The beam can propagate through the first substrate, then exits again with the angle Θ and is reflected at the second substrate at an angle Θ minus the wedge angle α. The reflected beam then has a new angle of incidence at the first substrate, which is reduced by 2α compared to the original Θ. This change in angle allows to induce a chromatic shift for dielectric coatings, e.g. long pass filter edges. In the experiments, a Semrock LP-1064-02RE [16] coating together with s-polarized 1030 nm laser light and an incidence angle of 34° allowed to capture essentially all light in the WOLIT. The beam then propagates multiple times back and forth as indicated in the drawing (Fig. 2 (b)), switches propagation direction and returns to its original propagation direction. To separate incoming and reflected laser light one may introduce a third angle δ between the incoming laser light and the plane of symmetry for the two substrates as depicted in Fig. 2 (a).

The total number of round trips or "order number" N depends on the ratio between 2α and Θ and can be calculated to $N = \frac{2\Theta}{2\alpha}$ or

$$\frac{1}{2\alpha} = \frac{N}{2\Theta}. \tag{1}$$

OSA CONTINUUM

The experimental setup is shown in Fig. 2 (c). The laser is coupled into a polarization-maintaining single mode fiber as a mode cleaner and is collimated to be used for the experiment. In order to apply a heterodyne phase detection, the incoming beam is split by an acousto-optical frequency modulator (AOM) into the original beam and into a second beam which is shifted in frequency by 100 MHz. The original beam is redirected through a lens (focal length f = 300 mm) to weakly focus (several 100 μm spot size) the laser light onto the WOLIT. The slightly tilted returning light is collimated by the lens and brought to interference via a beam splitter with the frequency shifted laser beam. The interference of the original beam and the frequency shifted beam results in a beating of the interference signal. The phase difference between the beating signal and the excitation signal of the AOM is proportional to the phase difference between the two interfering optical beams. Thereby, the change of the optical path length can be detected by measuring the phase shift of the beating signal [17]. The beating signal of the interfering beams is detected by an InGaAs-photodiode and the signal is mixed with a local oscillator into in-phase and out-phase components. The converted signals are digitized and the phase is recovered and unwrapped to overcome 2π jumps [18]. With the knowledge of the used laser wavelength the absolute change of the optical path length is recovered. With a beam sampler multiple reflection orders were projected onto a millimeter paper screen. By photographing the screen, the displacement D (compare Fig. 2 (c)) between succeeding reflection orders was documented. With the relation $2\alpha \approx \frac{D}{f}$ a deduction of the current reflection order (Fig. 5) was possible. The expected optical path length L after N mirror reflections can be calculated by summing up all segment lengths of the beam.

$$L = \sum_{i}^{N} l\,(\Theta_i) \tag{2}$$

The average change per reflection $\Gamma(\Theta)$ compared to the same amount of normal incidence reflections can be deduced by substituting the summation by integration and renormalization:

$$\Gamma(\Theta) = \frac{2}{2\Theta}\int_0^{\Theta} d\phi \frac{dl(\phi)}{dl(0)} \tag{3}$$

Such that the change in OPD equals a multiple of the positional change Δx (compare Fig. 2 (b)) of the actuated mirror $\Delta\mathrm{OPD} = 2N\,\Gamma(\Theta)\,\Delta x$. Due to the geometrical similarity of the optical path, the path difference $dl(\phi)$ with ϕ as intermediate angle of incidence can be expressed as:

$$dl(\phi) = \frac{2\,\Delta x}{\cos(\phi)} \tag{4}$$

This results in the approximation:

$$\Gamma(\Theta) = \frac{1}{\Theta}\int_0^{\Theta} d\phi \frac{1}{\cos(\phi)} = \frac{1}{\Theta}\ln\left|\tan\left(\frac{\Theta}{2}+\frac{\pi}{4}\right)\right| \tag{5}$$

This relation was used to implement highly dispersive optical elements by introducing a free-space angular-chirp-enhanced delay (FACED) [14]. An analogous calculation leads to the spatial displacement $\Delta r = 2N\,\xi(\Theta)\,\langle d\rangle$ of the beam in the WOLIT (compare Fig. 2 (b)). With $\langle d\rangle$ as the average distance between the substrates (compare Fig. 2 (b)).

$$\xi(\Theta) = \frac{1}{\Theta}\int_0^{\Theta} d\phi \tan(\phi) = -\frac{1}{\Theta}\ln|\cos(\Theta)|. \tag{6}$$

As also expirienced in FACED systems.

OSA CONTINUUM

3. Results

In order quantify the scale-ability of the induced optical phase shift, the maximum phase shift was determined with respect to the number of reflections. Therefore, a piezo attached with a 5 mm mirror attached was driven by a sinusoidal oscillating voltage with an amplitude of approximately 400 mV. This results in a small mechanical displacement Δx of the mirror and thereafter changes the OPD of the outgoing light with respect to the incoming light. By changing the wedge angle α between the edge filter and the mechanically oscillating mirror, the shift of the optical phase was increased proportionally to the number of reflections on the mirror of the folded beam. The phase-modulation was detected heterodyne by an InGaAs-photodiode and recorded by a software defined radio (SDR) device. The amplitude of the phase modulation was determined by fitting a sine function to the measured data. The phase modulation was measured at 10 different oscillation frequencies (10 kHz, 20 kHz,. . . , 100 kHz) of the piezo. In the range from 45 kHz to 75 kHz a mechanical resonance of the piezo was located. The dashed lines in Fig. 3 represent a fitted function of a simple model of a harmonic oscillator.

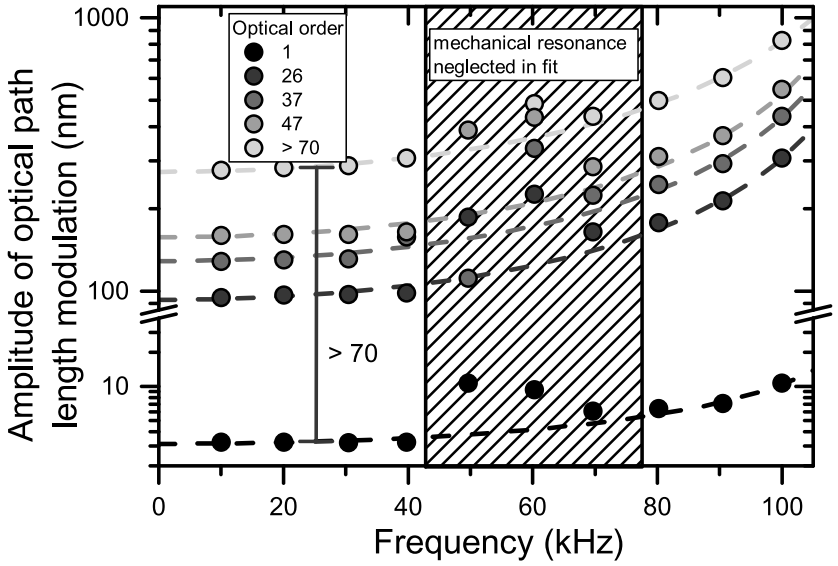

Fig. 3. Measured amplitude of the optical path modulation for five distinctive optical orders of the WOLIT. The modulation amplitude rises towards the first electrical resonance.

The resonance frequency of the fit function at 119 kHz corresponds to the first electrical resonance frequency of the piezo which was measured separately with an electronic vector analyzer. Data in the range of the mechanical resonance were neglected in the fit. As can be seen, the amplitude of the phase shift is increased by the order of optical reflection. This amplification of the OPD is independent from the applied frequency of the mechanical oscillation and surpassed the reference of a single reflection approximately 70-fold. The determination of the order was inaccurate at higher numbers. Therefore the highest order number can not be declared more precisely than > 70. This results into a modulation of the optical path of approximately one wavelength (1 μm) at a modulation frequency of 100 kHz. Transmission of the system at approximately 70th order was at 19 % with respect to the 1st order which corresponds to the expected 23 % overall transmittance due to reflection losses of 2 % per round-trip within the WOLIT dominated by the broadband HR coating of the mirror.

To properly correlate these findings to our theoretical predictions, the angular properties of the long pass filter were measured separately. A Fourier-Transform infrared spectrometer (FTIR)

OSA CONTINUUM

was used to measure the angular filter response. While maintaining s-polarization the angle of incidence was varied. The wavelength at 50 % transmission was plotted over the corresponding angle (Fig. 4).

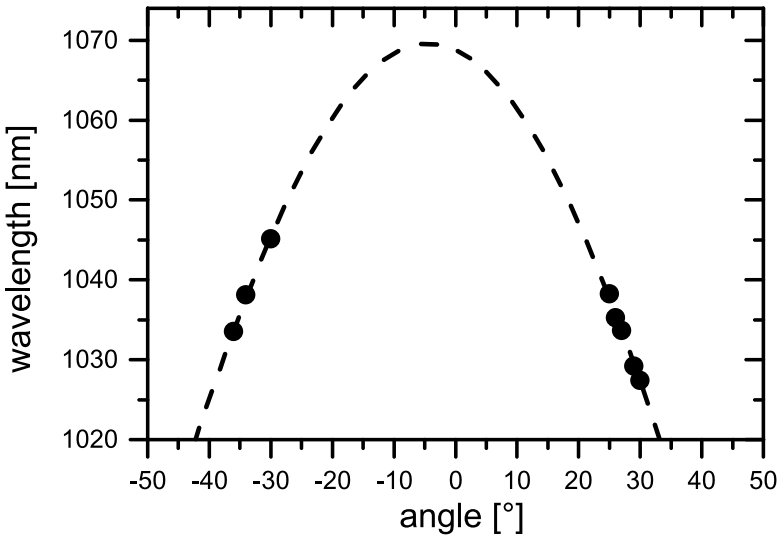

Fig. 4. Dependency of the spectral position of the filter edge on the angle of incidence [13] as measured (circles) with fitted model (dashed line).

By fitting the theoretical curve and the effective refractive index of the layered system with [13]

$$\lambda_e(\Theta) = \lambda_e(0^\circ)\sqrt{1 - (sin^2(\Theta/n_{eff}^2))} \tag{7}$$

the angle of incidence is expected to be 33.1° for the 1030 nm laser source.

The angle between two succeeding reflection orders (2α) was determined as described. The resulting reciprocal angles were plotted against the measurement number (Fig. 5) and via a linear fit an extrapolation to the absolute reflection order was possible. As depicted in Eq. (1) the slope of this curve of $(0.01476 \pm 0.00009)1/^\circ$ is the reciprocal of twice the angle of incidence. Therefore, the angle of incidence is deduced to be $33.9^\circ \pm 0.2^\circ$, which supports the results given by the FTIR spectra.

With this angle the relative phase amplification factor $\Gamma(34^\circ)$ (compare Eq. (5)) is expected to equal 1.064. Determining the slope of the phase amplification over the reflection order and relating this to the case of direct reflection results in a factor of 1.07 ± 0.04 which is in agreement with the theoretical prediction (Fig. 6).

OSA CONTINUUM

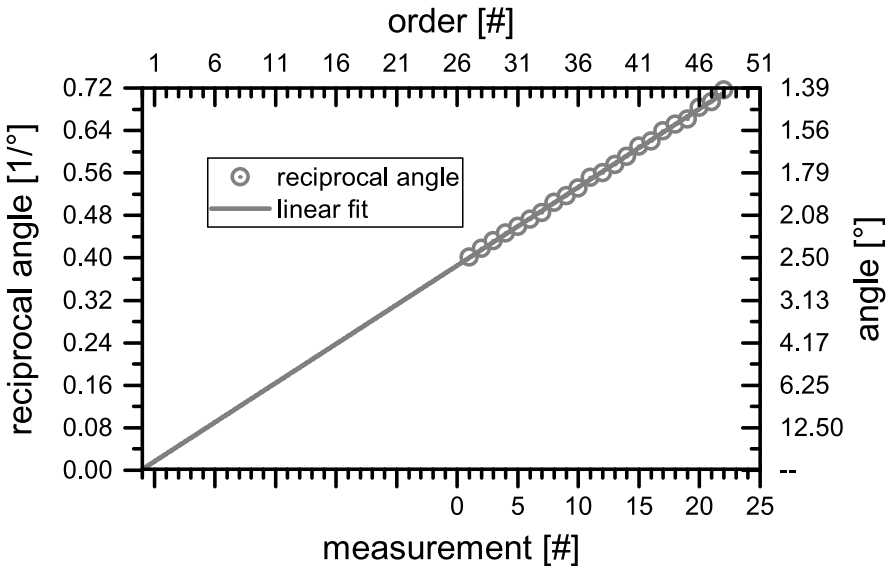

Fig. 5. Angle between to succeeding reflection orders over measurement number. An extrapolation to the order number (top x-axis) is introduced via a linear fit.

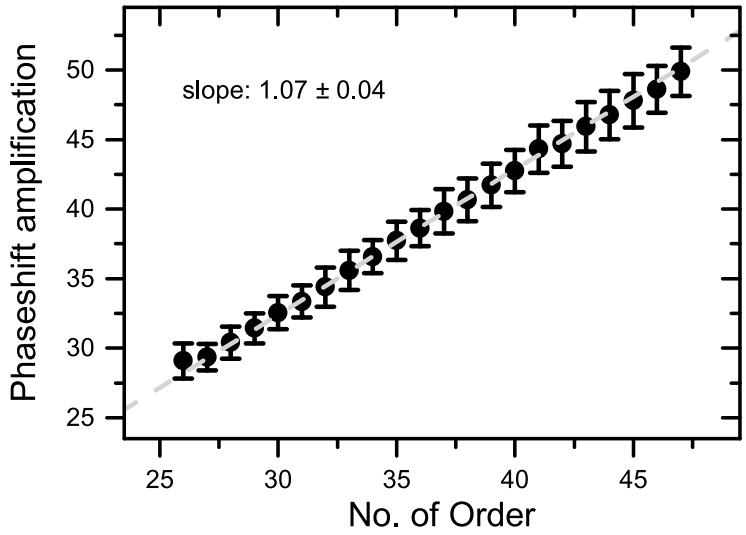

Fig. 6. The amplification of the phase shift with respect to the optical order of the WOLIT device. Order numbers higher than 47 are not shown due to the inaccuracy of the determination of higher order numbers

OSA CONTINUUM

4. Conclusion

This work describes and successfully demonstrates the suitability of a WOLIT as an OPD modulation device. In future work we plan to adapt enhanced piezo technologies [3,4] to overcome the described resonance effects. Furthermore, precision close loop operation has to be developed for substitution of our current phase shifters.

The overall OPD performance was increased more than 70-fold, while transmission of laser-light decreased to one fifth of the input power. Optimized mirror coatings are expected to eventually reduce overall losses to several per cent. Succeeding this experimental verification, further areas of application are imaginable. This includes improved mechanical or micro-mechanical scanners [19], compact multi-pass absorption cells, light pressure amplification, precise surface flatness inspections, atomic force microscopy [20], laser microphones, accelerometers and even laser cooling [21]. For a fast implementation in other projects a list of possible commercial filters with corresponding wavelength which are theoretically suitable as a WOLIT filter, is shown in Table 1.

Table 1. Selection of alternative commercial filters (Semrock) with corresponding wavelength. The "unpol" column contains filters without polarization sensitivity and the "s/p split" shows polarization sensitive types.

wavelength [nm]	unpol	s/p split
1064	TLP01-1116	
1030		LP02-1064RE
632		LP02-664RU
532	TLP01-561	LP02-561RE
450		LP02-473RE
405		LP02-442RE

Acknowledgments

We want to thank our colleagues supporting us in the preparation to these experiments and Samantha Rose Siegert and Christian Vorholt for proof reading the manuscript.

References

1. Y. Y. Jiang, A. D. Ludlow, N. D. Lemke, R. W. Fox, J. A. Sherman, L. S. Ma, and C. W. Oates, "Making optical atomic clocks more stable with 10–16-level laser stabilization," Nat. Photonics **5**(3), 158–161 (2011).
2. B. Willke, K. Danzmann, M. Frede, P. King, D. Kracht, P. Kwee, O. Puncken, R. L. Savage, B. Schulz, F. Seifert, C. Veltkamp, S. Wagner, P. Weßels, and L. Winkelmann, "Stabilized lasers for advanced gravitational wave detectors," Classical Quantum Gravity **25**(11), 114040 (2008).
3. T. C. Briles, D. C. Yost, A. Cingöz, J. Ye, and T. R. Schibli, "Simple piezoelectric-actuated mirror with 180 kHz servo bandwidth," Opt. Express **18**(10), 9739 (2010).
4. D. Goldovsky, V. Jouravsky, and A. Pe'er, "Simple and robust phase-locking of optical cavities with > 200 KHz servo-bandwidth using a piezo-actuated mirror mounted in soft materials," Opt. Express **24**(25), 28239 (2016).
5. Y.-S. Jin, S.-G. Jeon, G.-J. Kim, J.-I. Kim, and C.-H. Shon, "Fast scanning of a pulsed terahertz signal using an oscillating optical delay line," Rev. Sci. Instrum. **78**(2), 023101 (2007).
6. G.-J. Kim, S.-G. Jeon, J.-I. Kim, and Y.-S. Jin, "High speed scanning of terahertz pulse by a rotary optical delay line," Rev. Sci. Instrum. **79**(10), 106102 (2008).
7. M. Skorobogatiy, "Linear rotary optical delay lines," Opt. Express **22**(10), 11812 (2014).
8. A. Roggenbuck, K. Thirunavukkuarasu, H. Schmitz, J. Marx, A. Deninger, I. C. Mayorga, R. Güsten, J. Hemberger, and M. Grüninger, "Using a fiber stretcher as a fast phase modulator in a continuous wave terahertz spectrometer," J. Opt. Soc. Am. B **29**(4), 614 (2012).
9. D. A. Henderson, C. Hoffman, R. Culhane, and D. Viggiano III, "Kilohertz scanning all-fiber optical delay line using piezoelectric actuation," Fiber Opt. Sens. Technol. Appl. III **5589**, 99 (2004).
10. D. R. Herriott and H. J. Schulte, "Folded optical delay lines," Appl. Opt. **4**(8), 883–889 (1965).
11. P.-L. Hsiung, X. Li, C. Chudoba, I. Hartl, T. H. Ko, and J. G. Fujimoto, "High-speed path-length scanning with a multiple-pass cavity delay line," Appl. Opt. **42**(4), 640–648 (2003).

OSA CONTINUUM

12. Y. Pan, E. Lankenou, J. Welzel, R. Birngruber, and R. Engelhardt, "Optical coherence-gated imaging of biological tissues," IEEE J. Sel. Top. Quantum Electron. **2**(4), 1029–1034 (1996).
13. M. Lequime, "Tunable thin film filters: review and perspectives," Adv. Opt. Thin Films **5250**, 302 (2004).
14. J.-L. Wu, Y.-Q. Xu, J.-J. Xu, X.-M. Wei, A. C. Chan, A. H. Tang, A. K. Lau, B. M. Chung, H. C. Shum, and E. Y. Lam, *et al.*, "Ultrafast laser-scanning time-stretch imaging at visible wavelengths," Light: Sci. Appl. **6**(1), e16196 (2017).
15. A. J. Fleming, "A review of nanometer resolution position sensors: Operation and performance," Sens. Actuators, A **190**, 106–126 (2013).
16. T. Erdogan and L. Wang, *Semrock White Paper Series. Semrock Versa Chrome. The First Widely Tunable Thin-Film Optical Filters* (2014).
17. W. Puschert, "Optical detection of amplitude and phase of mechanical displacements in the Åstrom range," Opt. Commun. **10**(4), 357–361 (1974).
18. T. R. Judge and P. J. Bryanston-Cross, "A review of phase unwrapping techniques in fringe analysis," Opt. Lasers Eng. **21**(4), 199–239 (1994).
19. T. Bifano, "Adaptive imaging: MEMS deformable mirrors," Nat. Photonics **5**(1), 21–23 (2011).
20. D. Rugar, H. J. Mamin, and P. Guethner, "Improved fiber-optic interferometer for atomic force microscopy," Appl. Phys. Lett. **55**(25), 2588–2590 (1989).
21. S. Gigan, H. R. Böhm, M. Paternostro, F. Blaser, G. Langer, J. B. Hertzberg, K. C. Schwab, D. Bäuerle, M. Aspelmeyer, and A. Zeilinger, "Self-cooling of a micromirror by radiation pressure," Nature **444**(7115), 67–70 (2006).